Experimental characterization of pedestal density fluctuations and correlation with pedestal evolution on JET

Daniel José Lopes da Costa
daniel.l.costa@tecnico.ulisboa.pt

Instituto Superior Técnico, Lisboa, Portugal

March 2021

Abstract

Controlled nuclear fusion is a safe and abundant energy source that may help balance the energy mix of future generations. Currently, the best results are obtained in tokamaks that magnetically confine a plasma heated to temperatures over 100 million degrees Celsius. The preferable mode of operation for tokamaks is the H-mode, that although provides improved confinement, is worrying because of the emergence of instabilities such as Edge Localised Modes (ELMs). Not only do these events damage the wall components, but they may also inhibit the plasma from reaching the critical densities and temperatures required for fusion. Understanding the instabilities causing ELMs is rather important and was one of this thesis' objectives. A set of three discharges from JET were analysed through a microwave reflectometry system operating in Doppler mode. This diagnostic allows studying density fluctuations, δn_e, at the plasma edge. In this work different numerical methods were applied and a method was developed to characterize a coherent mode in δn_e. The focus of the study was on both understanding the general behaviour of a specific mode as well as determining its location. We noted that mode intensity was more correlated with density evolution rather than temperature. We characterised the mode between ELMs with frequency around 80 kHz and located around the upper half of the steep gradient region. Its frequency tended to decrease as the radius increased.
Keywords: ELM, H-mode, Reflectometry, density fluctuations, plasma.

1. Introduction

Controlled nuclear fusion may be a reliable alternative in the near future to the non-renewable and polluting fossil fuels. There are many configurations in order to achieve it, but the most promising one for a fusion reactor is the tokamak. This machine consists of a torus shaped vessel in which a Deuterium and Tritium gas mix is elevated to considerably high temperatures. The D-T elements are the preferable option for fusion due to the conditions needed to achieve it and because they provide a high energy output reaction, given by 1.

$$\mathrm{D} + \mathrm{T} \rightarrow \alpha + \mathrm{n} + 17.6\ \mathrm{MeV} \tag{1}$$

Deuterium and Tritium are isotopes of hydrogen that when confined at high enough density and temperature, for a minimal period of time, can overcome the inter-particle Coulomb potential and fuse together. The products of the reaction are α-particle (He^{2+}), and a neutron with 3.5 MeV and 14.1 MeV of kinetic energy, respectively. The high temperatures fusion requires cause the gas mix to turn into a plasma, a gas of ions and free electrons that have collective behavior. Tokamaks use appropriate magnetic fields to confine the plasma and to reduce the interaction with the vessel walls.

There are different regimes in which a reactor can work depending on external heating and the plasma configuration. The low confinement mode (L-mode) used to be the regime in which most reactors worked until the high confinement mode (H-mode) was discovered. This H-mode is characterized by different experimental observations: the overall increase of the pressure and the appearance of a steep pressure gradient at the edge; the emergence of instabilities named Edge Localized Modes (ELMs); an abrupt reduction in heat and particle transport at the edge, provided by an Edge Transport Barrier (ETB). The access to the H-mode is attained by first reaching the L-mode and then after a certain level of external heating is surpassed, named threshold power (P_{LH}), the L-H transition occurs. Although this H-mode has clear advantages in advancing fusion, the buildup of a steep edge pressure gradient accompanied with the current gradients are drivers of instabilities like ELMs. These events are concerning in tokamaks as they limit energy confinement and destroy the pedestal periodically. They also produce large heat pulses on the divertor and first wall materials that increase sputtering and may cause permanent damage. ELMs are the subject of an intense experimental characterization since they are complex phenomena and no first principles theory exists describing them [7]. Understanding ELMs will help develop techniques that mitigate or control them. How ELMs develop is correlated to various instabilities that can form at the plasma edge. The Peeling Ballooning Modes (PBMs) may explain some types of ELMs. These are the combination of ballooning modes caused by exceeding a certain pressure gradient and by peeling modes that emerge after a certain edge current density is surpassed. Another instability that limits the edge pressure gradient are Kinetic Balloooning Modes (KBMs), these are the kinetic analogues of ideal ballooning modes [3], occurring parallel to magnetic field lines which are not considered in ideal MHD equations. Characterizing instabilities in their inter-ELM evolution and relating them to edge plasma parameters like electron temperature and density may help unravel their origins.

In this thesis, we describe and analyse an instability

detected at the steep density gradient region in the context of type-III ELMs. The instability is mostly studied in the context of these events using Doppler Reflectometry and magnetic coils.

The paper is organized as follows: this introductory chapter has an overview of nuclear fusion in tokamaks; followed by an exposition of types of discharges analysed and the different diagnostic tools used; then the developed methods used on the diagnostic data to extract relevant information are explained; succeeded by the experimental results of the mode and some observations on these discharges; and finally the conclusions are gathered and possible future work mentioned.

2. Experimental setup

Over the years, several L-H threshold experiments were performed on JET to investigate the dependencies of the P_{LH} [2, 4]. From these, three representative discharges are analysed here. The discharge 84733, with a toroidal field $B_t = 2.4$ T and plasma current $I_p = 2$ MA, was used primarily to characterise the evolution of a mode associated with ELMs and relate that evolution with plasma parameters. The other two, the #86469 and #86470, with higher $B_t = 3$ T and $I_p = 2.5$ MA, had the additional aim of trying to localise this mode. In all of these discharges external heating was provided exclusively by Neutral Beam Injection (NBI). NBI is a method used to increase the temperature through injection of high energy neutral particles.

The mode is detected in the density fluctuations, δn_e, observed through a radial correlation reflectometer (CR). The JET CR used in this work contains two X-mode fast frequency hopping channels launched from the Low Field Side (LFS) mid-plane and designed for normal incidence [6]. However, in the studied discharges, there is a deliberate vertical shift of the plasma column that causes a small oblique angle between the incident beam and the cut-off magnetic surfaces. This way the diagnostic operates as Doppler Reflectometry. This system provides heterodyne signals of in-phase and quadrature-phase (I.Q.) each with information about the amplitude and the phase. The CR signals are recorded them at a sampling rate of 2 MHz.

Locating where the probing frequency (PF) of CR is measuring is done using electron density profiles obtained with the fast sweep reflectometry. These n_e profiles also give information on how steep density gradient region is. This diagnostic has been designed to have a repetition interval as low as 15 μs but in order to monitor a whole discharge is often set at around 1 ms time resolution.

The system of fast Mirnov coils at JET complement the detection of instabilities. In this work, 4 coils were used, one in the High Field Side (HFS) belonging to the Inner Coils group (I803); and three positioned in the LFS, with two in the Poloidal Limiter Coils group (P802B and P803B), and another in the Toroidal array (T001) [5]. All the coils have a sampling frequency of 1 MHz, except T001 with 2 MHz.

Plasma parameters at different radii can be correlated with mode evolution. Electron temperatures are obtained using ECE through a multi-channel (96 channels) radiometer that gives reliable measurements with a sampling frequency of up to 5 kHz. The far infrared (FIR) diagnostic provides electron line-averaged densities every 15 ms along specific lines of sight.

Transport and ELMs were monitored using the Be II and D_α signals. The Be II signal results from the emission of sputtered Be particles from the JET Beryllium walls, due to increased transport in the edge plasma. Spectrometers detect this radiation at a sampling frequency of 10 kHz. D_α radiation is emitted by an excited deuterium after a $n = 3 \rightarrow n = 2$ electron transition. This radiatiom was measured using photomultipliers viewing the divertor region. It was sampled at a frequency of 10 kHz.

3. Methodology

Tools were developed to more easily analyse the experimental data.

3.1. ELM and Sawtooth detection

Firstly, it was important to develop methods that identify events such as ELMs and sawteeth so we could correlate them to the evolution of the mode of interest. An algorithm was developed to signalize their start by analyzing the Be II signal, the blue line in figure 1. An algorithm was defined that smoothened the data in order to identify the maximum of ELM events (red points). But since the beginning of ELM events is more important we identified the ELMs start by calculating the difference between a Be II signal shifted by t_{step} and the original signal. The t_{step} is set so **Be II [t+t_{step}]-Be II [t]** is maximized for most ELMs at its beginning at $t_{step} = 2.5$ ms and the resultant quantity is plotted in green in figure 1. From this modified signal, the maxima were identified (black points) and the ones closest to each ELM peak were selected as an ELM onset (green points).

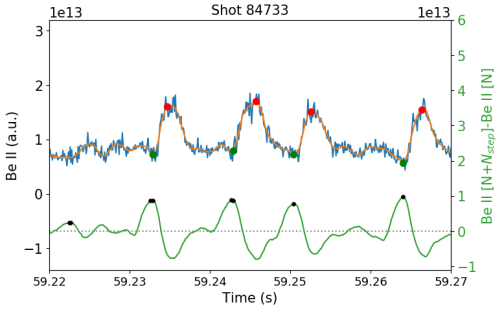

Figure 1: ELM detection algorithm

Sawteeth were best identified by monitoring the falls at the core electron temperature. They were obtained by calculating a difference between core temperatures separated by 3 consecutive data points. Visible in the figure 2, in blue, is the typical temporal evolution of core temperature, and the green line is the difference of this temperature which has identifiable peaks that mark the drop, that were marked with red dots.

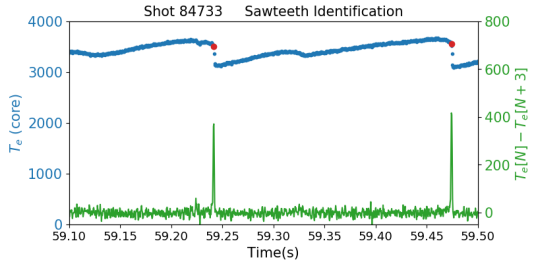

Figure 2: Example of detected Sawteeth

3.2. Electron density profiles

The fast sweep reflectometry system provided profiles of electron density and the correspondent PFs that were used to localize the Doppler reflectometry measurements. This was done by checking the closest available profile in time and then for each profile the location of the closest PF used by the CR is estimated. Density profiles measured by reflectometry are highly dynamic having often fluctuations that may not be relevant for our analysis. Therefore averaged density profiles of roughly stationary periods were obtained. These averaged profiles show often a clear radial shift between them as the steep gradient region is not aligned. A method was developed to align these profiles based on the identification of the inflection point. All the profiles were shifted so the inflection points were aligned with the one from a representative density profile of JET.

3.3. Modified Welch Method

The main aim of this work is to investigate coherent modes using Doppler refletometry data. The I=A cos(ϕ), Q=A sin(ϕ) signals provided by this diagnostic store valuable information on density fluctuations in both the amplitude, A, and the phase, ϕ, of these signals. A way to combine both is to define a complex signal $Ae^{j\phi} = I + jQ$. Using this complex signal to develop a spectrogram, like the one in figure 3, allows the tracking of coherent fluctuations in time.

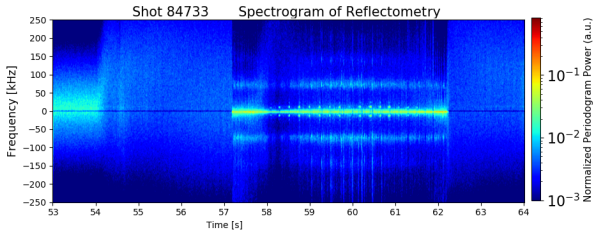

Figure 3: Spectrogram of discharge 84733

In the three discharges studied, the Power Spectral Density in H-mode is roughly symmetric. So, for this work, only positive frequencies are considered.

A way to improve the amplitude estimation of each spectral component of a PSD is by using a modified Welch method. This method takes each segment from a normal spectrogram and subdivides it into many smaller segments with 50% of the points overlapping. After applying a Hanning window function, it calculates the DFT for each smaller segment and averages the PSDs. We also overlapped 50 % of the points between consecutive PSDs so to have higher time resolution. The resulting power spectrum is built with reduced uncertainty compared to a normal PSD. However, by reducing the length of each segment causes the frequency resolution to decrease. Because the amplitude of the signal often varies significantly between PFs along the discharge, a normalization of the PSD with a corresponding PF total power is done to facilitate the analysis.

3.4. Determination of the mode amplitude and width

The correct determination of the amplitude of the coherent modes is crucial in this thesis. There was a varying background component with an amplitude decaying roughly with $1/f^2$ in each PSD that affected the mode characterisation. This baseline was subtracted by fitting a somewhat versatile function like the equation 2.

$$y = \frac{a}{(f-c)^2} + b + df \tag{2}$$

where y is the power spectrum and f is the frequency. The constants a,b,c and d are free parameters to be fitted for each PSD.

When trying to fit the PSDs, the existence of modes made it difficult as they would induce the fit in error and the baseline was overestimated. These frequency ranges where the modes existed were ignored as illustrated in figure 4 with the vertical dotted red and green lines. The baseline was determined by a first fit with the points outside the frequency ranges, represented by the red line. A second fit using the points below the first fitted function was done again, shown by the green line. This way the fitted function would be closer to the visible baseline.

Having the baseline calculated, it was removed from the PSDs as shown in figure 5. The new PSD improved on mode characterization. The study of the modes was done in frequency ranges that allowed to track one mode in each interval. Based on the typical PSD components, we defined them as seen in figure 5, in a range of 5-50 kHz, 50-100 kHz, 100-150 kHz and from 150 kHz onwards. In each interval we carried out a peak finding algorithm resulting in the points marked in black. The mode base is attained by checking when the PSD is equal to zero. These points are signaled in red and set the width of the mode. Using this data, it was possible to define three fundamental characteristics that outline mode behaviour:

- The width of the mode, in frequency.
- The frequency weighted by the PSD (Mean freq.), calculated with an weighted average of the frequency by the PSD, along the width of the mode.
- The intensity of the mode, the integrated power along the width of the mode.

These three quantities were estimated along the discharge so the modes could be tracked.

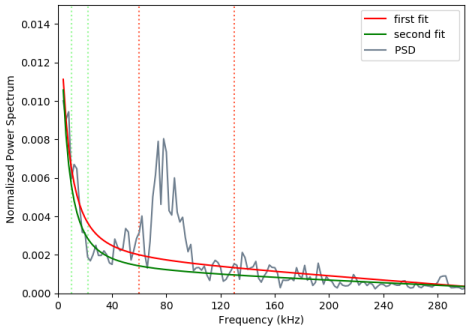

Figure 4: Baseline detection

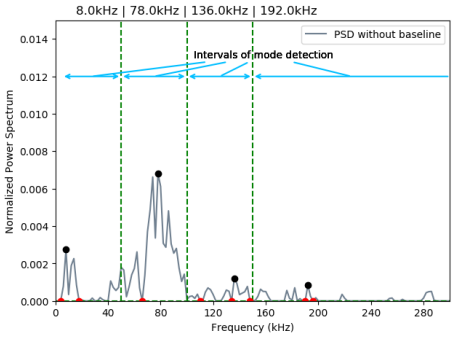

Figure 5: Power spectrum without baseline and mode detection

4. Results

4.1. Temporal evolution along the discharge

The main parameters needed to study the discharges are illustrated for #84733 in figure 6. In plot a), a simple spectrogram of the Doppler Reflectometry signal is presented for an overview of the plasma evolution. In plot b) we have the plasma stored energy, W_p, (in blue) and the heating power, P_{NBI}, (in red). ELM identification is done with the help of signals Be II (in blue) and D_α (in red) plotted in c). The D_α helps signalise the confinement mode of the plasma, as well as identify important small oscillations that affect the coherent mode. In order to keep track of the oscillations, the spectrogram of the D_α is developed in plot d). The temperatures from the ECE are also plotted for different regions of the plasma in e), with the respective locations shown in the legend. The interferometry system provided the line-averaged densities plotted in f). These are of the core (in blue) and the edge (in red) plasma. Finally, in plot g), the spectrogram of a LFS coil (T001) is shown, developed similarly to the spectrogram of Doppler Reflectometry.

An overall description of this discharge starts at the L-H transition, illustrated in figure 6, at t=57.2 s. Its trigger seems to be related with the increase in the P_{NBI}. The transition is characterised by an immediate fast decrease of D_α radiation and later by the emergence of ELMs. Also noticeable is the increase of plasma parameters like density, electron temperature and plasma stored energy associated with the increased confinement of H-mode. In the D_α spectrogram, the surfacing of oscillations at low frequency clearly mark the transition. In all discharges the P_{NBI} stays just above the L-H transition and the ELMs are most likely type-III.

The evolution of the plasma parameters is affected not only by ELM events but also by sawteeth. They are clearly identifiable through the abrupt periodic decreases of the electron temperature and line-averaged density most close to the core, Te_{88} and $n_e(core)$.

In the spectrogram of reflectometry in #84733, a coherent mode around 70-90 kHz is visible with varying intensity and affected by ELM events, this is the mode of interest that was studied. In all discharges this mode is present.

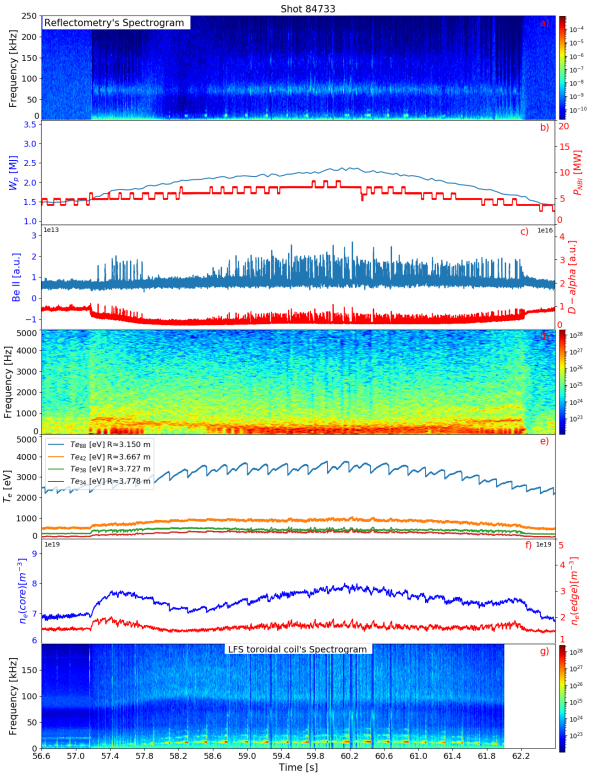

Figure 6: Evolution of Discharge 84733. a) Reflectometry spectrogram, b) plasma stored energy and NBI power, c) Be II and D_α signals, d) D_α spectrogram, e) electron temperatures, T_e, at different radial positions , f) electron line-averaged density, n_e, at the edge and at the core of the plasma, g) coil T001's spectrogram

Whenever an ELM occurs, the Be II and D_α signals help identify it, in figure 7 we have some examples of ELMs and how they affect the plasma parameters. The D_α has low frequency oscillations that are present throughout the discharge. The electron temperature evolution between ELMs varies along measurement location, visible in figure 7. The temperature profile has a pedestal similar to the density profile but not as steep. Te_{88} is measured very close to the core plasma and show a sawtooth event at t=57.425 s. Te_{38} and Te_{34} are on the top of the pedestal and at the middle of the steep density gradient region. They have a very clear correlation and evolution affected by the ELMs. By being

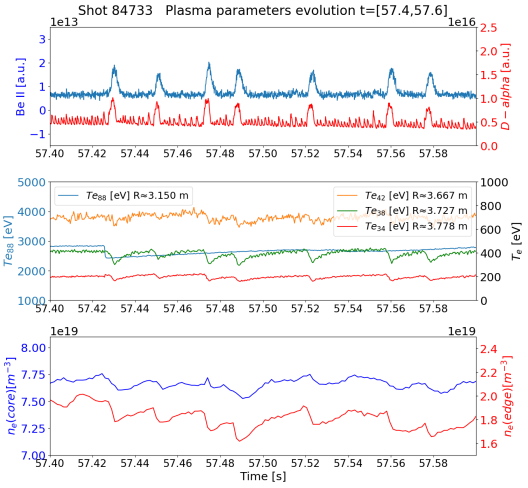

Figure 7: Example of set of ELMs in the Be II and D_α's signals. Also plotted are the temperatures at different radii (the scale of each axis is set for temperatures in closest legend) and electron line-averaged densities, n_e.

at the top of the pedestal, Te_{38} is the most sensible to the relaxation caused by the ELM to the temperature profile, it was chosen to correlate to the mode evolution. The line-averaged densities have abrupt drops in value after ELM events and usually have a steady recovery until the next one. Because these events occur near the pedestal, the edge's chord density is more reactive than the core's.

4.2. Reflectometry and Magnetic coils characterization of measured fluctuations

The analysis done for the mode of interest will focus on reflectometry data measuring δ_{n_e} complemented by the input from Mirnov coils to study associated magnetic fluctuations. Using them, the characterisation of this mode is facilitated through determination of its intensity, frequency and width.

Density fluctuations at a fixed layer

In #84733, the master channel of the CR was set to launch a single frequency, shown in table 1, that led to the plot a) in figure 6.

# Shot	# PF	PFs (GHz)	PF t_{step} (ms)
84733	1	73.44	0
864(69/70)	1	73.5	25
	2	75.5	
	3	77.5	
	4	79.5	
	5	81.5	
	6	83.5	
	7	85.5	
	8	87.5	

Table 1: Emitted frequencies by the hopping reflectometry system and their time step for different discharges

Although Doppler reflectometry is normally used to measure rotation velocities of the turbulence, for the H-mode, turbulence is strongly reduced by the E×B shear. As illustrated in figure 6, after the L-H transition at t=57.2 s, the Doppler signal is very weak, giving opportunity for modes to dominate and become visible in the spectrogram. A general analysis of the spectrogram show the presence of a mode at 70-90 kHz. This coherent mode is only present in the H-mode and seems to be correlated with ELM events. It is broad in frequency, disappears whenever an ELM happens and exists intermittently along the discharge. After looking more in-depth to this intermittent behaviour, the reason behind it is visible in both the reflectometry and magnetic's spectrogram of figure 8. With the overplotted D_α in these spectrograms, it seems that the smaller oscillations visible in this signal are the cause of the mode disappearing periodically. Whenever these pulsations in the D_α reach their peak, there is an overall reduction of activity and disappearance of the mode in the CR spectrogram. In the magnetic signals, these oscillations cause momentary broadband fluctuations in the spectrogram that range up to 200 kHz in some coils. These D_α pulsations emerge in the H-mode with regular behaviour up to 1 kHz, as W_p rises they reduce in frequency and in some intervals seem to evolve into type-III ELMs. These characteristics accompanied by their appearance just above the L-H threshold indicate they may be Limit Cycle Oscillations (LCO). Observed in many other machines [1], LCOs are regular pulsations in the low kilohertz range that occur at the edge of the plasma. Although these oscillation may have interesting physics, they complicated the analysis of mode characteristics, so in order to have a more robust estimate of the mode evolution, we implemented a spectrogram using a modified Welch method for all the studied discharges. The number of windows and their period were set to have a temporal resolution of 1.25 ms and so that the repetitive disappearing behaviour would merge with the mode, so that it would be more continuously analysed.

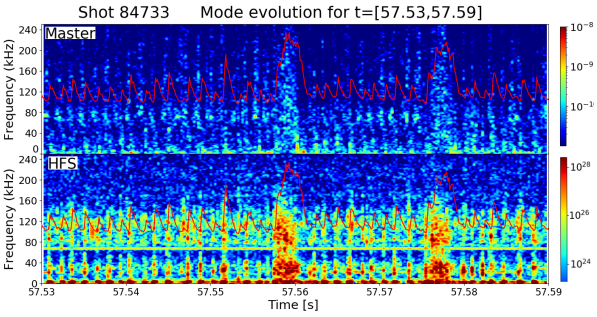

Figure 8: Spectrogram of the master signal of CR and the HFS coil(I803) with superimposed D_α signal (in red)

Also noticeable is that the mode of interest in the CR varies intensity along the discharge as the edge density varies. After comparing the electron density profiles of regions where the mode is faint to when is strongest in the CR, we noticed that what differs is the region being probed. When the mode is strongest, the electron density profile is steep and the CR is probing the top of the steep gradient region. When the mode is very weak the

density profile is smaller and the CR is probing more inside the plasma. We can relate this observation with the noticed mode intensity correlation with the edge's line-averaged density. The mode intensity increasing with edge density may be due to a temporary lower profile after ELM events. The probing region changes to more inside the tokamak and lowers the mode intensity and as the density profile recovers the CR starts to scan again around the steep gradient region, where the mode seems to be localised and is stronger. We can't be sure that the density/temperature gradients don't play a part by probing a single density layer which is why the other discharges probe the plasma at different radii and will help answer this question.

Some ELMs a few seconds after the L-H transition are presented in figure 9 in plot a). In it are also plotted the evolution of the edge density and temperature, in plot b), as well as the modes detected in three frequency ranges, in plot c), d) and e). The width of the mode is also displayed by a vertical line. Different frequency ranges have a certain color to identify their mode. The intensity along time for each frequency range is marked by the magenta points. Note that due to the background fluctuations in the spectrum, even after removing the baseline there is a minimum detectable mode amplitude (horizontal line in figure 9). The minimum intensity for a mode to be detected and plotted was set at $I_{min} = 30$. For every instant, the most intense mode from the frequency ranges is marked in orange. We attributed different symbols if the mode's width is shared or not with other modes:

- $\triangle$ - the mode's base is shared with the higher frequency range, the mode plotted above
- $\triangledown$ - the mode's base is shared with the lower frequency range, the mode plotted below
- $\Diamond$ - the mode is so wide that shares the base with the higher and lower frequency ranges
- $\circ$ - the mode's width is not shared with other modes

The mode of interest is detected with a frequency between 70-80 kHz with around 30 kHz width, it stands out in the mode detection of reflectometry signal in plot d). It disappears momentarily with an abrupt intensity loss whenever an ELM occurs followed by a recovery to pre-ELM intensities that seems to be somewhat related to the evolution of the edge density. Once the intensity of the mode stops increasing, it usually fluctuates over a value until the next ELM.

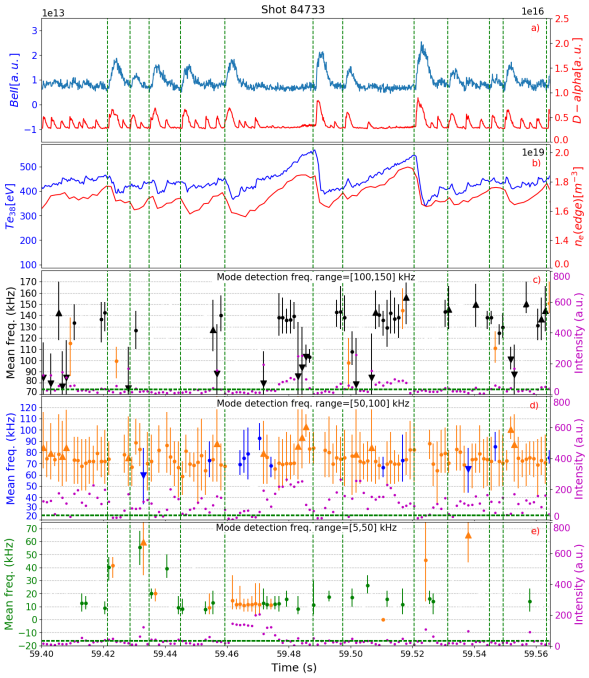

Figure 9: Mode evolution between ELMs. a) Be II and D_α signals, b) Te_{38} and n_e(edge), frequency of the modes and their intensity (in magenta) identified in different frequency ranges: c) 100-150 kHz; d) 50-100 kHz; e) 5-50 kHz.

There are inter-ELM periods without the D_α oscillations that allow for a better characterisation of the mode. In these occasions, the recovery of the mode after the ELMs seems to follow the edge line-averaged density, rather than the edge temperature, Te_{38}. This is illustrated in figure 9. The mode seems to saturate in intensity according to the saturation of edge density at times like t=[59.465,59.485] and t=[59.5,59.52]. After this saturation the mode behaviour until the next ELM is more arbitrary. In figure 10, the reduction in the D_α oscillations in t=[59.471,59.487] allows to observe a mode in the magnetic signals very similar in frequency and behaviour to the one in reflectometry. This magnetic mode appears mostly for these specific ELMs and overall is not visible in the spectrogram of the toroidal coil in figure 6. These more intense ELMs have the particularity that the 70-80 kHz mode becomes very well defined, a few instants before the disruptive event. This happens in both the reflectometry and magnetic signals. In the reflectometry signal these modes are so intense that a second and sometimes third harmonics are visible. These seem to be artificial as they do not exist in the magnetic signal and their origin may be due to the complexity of the I.Q. signals. From inspection of some examples, there is a general behaviour of the mode, between ELMs, that has 2 associated phases. We can see an example of this in figure 10 with the transition between the two stages being marked by a vertical green line. There is an initial phase, at t=[59.475,59.484] s, where the mode becomes increasingly strong with intensities above the usual. Followed by a phase, at t=[59.484,59.488] s, where the mode reduces intensity,

definition and becomes less coherent and sometimes disappears until the ELM event. After observing more of these intense ELMs, the onset of the second phase can usually be correlated with the saturation of the edge density and with an increase of D_α fluctuations at t=59.484 s. The mode does not exist in the master reflectometry signal before some of these ELMs, suggesting that either they may not be correlated or that the mode moves location after this change. Looking at the magnetic signals' spectrograms, this mode only exists in the LFS. There are no signs of it existing in the HFS coil, suggesting a ballooning character of the mode.

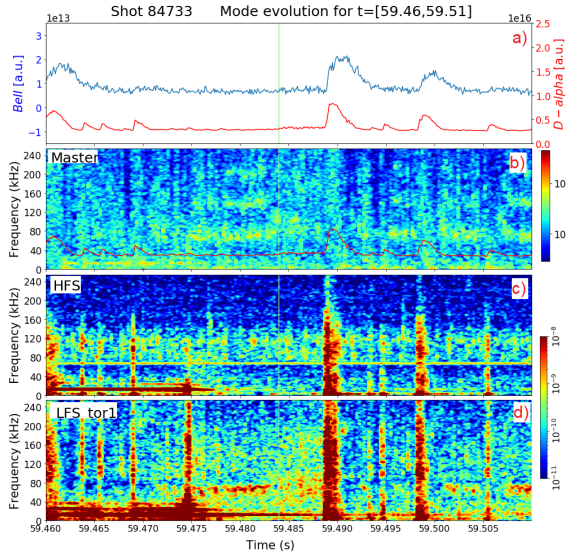

Figure 10: Detailed analysis of intense ELM. a) Be II and D_α signals, b) spectrogram of the master channel, spectrograms of magnetic coils signals: c) I803 (HFS), d) T001 (LFS_tor1)

After comparing the mode of interest of the reflectometry and LFS magnetic signals, a frequency shift of the mode by about 5 kHz to smaller values was evident in the magnetic signals. The reasoning behind this shift could be because the mode is not localised to a single plasma layer but is instead distributed across the plasma over a radius range. Considering the magnetic perturbations decay with 1/R we could assume the outer layers of the mode to be most responsible for the magnetic mode identified in the coils. If these layers are slower than the layer identified by the CR that would explain the mode being identified at a lower frequency.

In the reflectometry's spectrogram, another coherent mode is noticeable at 10 kHz at t=[59.464,59.470] s in figure 9 d). It exists just before some stronger sawtooth events occur in the CR and is also present in the magnetic signals, more in the LFS than HFS. They exist in the magnetic signals throughout the discharge, with mode harmonics when the mode is strongest. The mode disappears briefly after sawtooth events usually marked by the Te_{88}.

Density fluctuations in multiple layers

The reflectometer allows, for each channel, to be preprogrammed with a specified launch frequency pattern. The chosen frequencies are repeated continuously throughout the discharge, allowing a radial scan of the measurement location. For the discharges 86469 and 86470, one of the reflectometer channels (master) was set to a 8 point frequency sweep. Each frequency had a duration of 25 ms, with the full sweep taking 200 ms. The set of frequencies used are in table 1. By changing the layer being observed every 25 ms, it allows to identify the mode's frequency and intensity along the radius. The resultant spectrograms of this launch frequency pattern are in figure 11, and it is noticeable the periodic change of fluctuations spectra as the different plasma layers are probed.

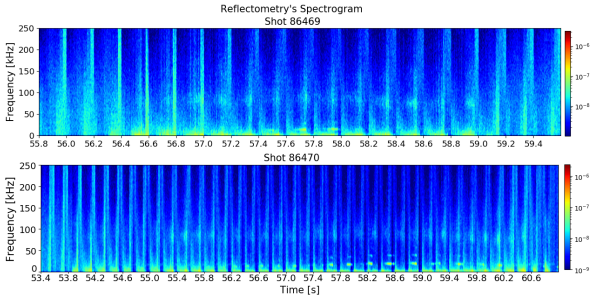

Figure 11: Reflectometry spectrogram of discharges 86469 and 86470).

A similar mode to the previous discharge also appears in the reflectometry spectrograms of these two discharges. Initially very wide, it varies the frequency around 70-100 kHz and seems to emerge after the H-mode is achieved. In both discharges, the mode is better defined for higher values of edge density. There are no signs of any magnetic fluctuations that can be associated with this mode. A particular behaviour that is worth noticing is that mode frequency seems to vary with the P_{NBI} along the discharges. In the discharge 86469, the evolution of the mode a few moments after an increase in P_{NBI} shows a rise in the frequencies of the mode from 70-90 kHz to 80-100 kHz. When the P_{NBI} is reduced, 0.2 s after the change the mode drops back to frequencies of 70-90 kHz. There is a tendency of the mode frequency to increase and decrease along with the P_{NBI}, this trend was also verified in the discharge 86470. This dependence of the mode frequency on the heating power occurs because an increase in P_{NBI} causes a higher rotation of the plasma, increasing the mode frequency.

The mode associated with the sawtooth event, mentioned in the discharge 84733, is also present in the reflectometry signal for these discharges and also varies in frequency with P_{NBI}. The discharge 86470 has more intense sawteeth which translates to an associated mode of higher intensity. Usually, when present in the reflectometry signal, a decrease in the strength of the mode at 70-100 kHz is observed, which is illustrated in figure 12. After the sawtooth occurs, the mode at 70-100 kHz increases in intensity immediately after to normal

values. This phenomenon happens in other intervals of the discharge 86470 and 84733, its cause may be a magnetic instability associated with the sawtooth affecting the main mode being studied.

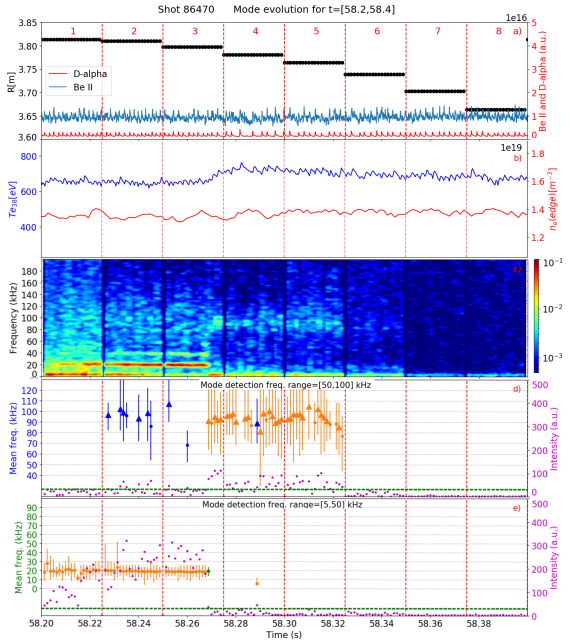

Figure 12: a) Radial location of the PF and signals of Be II (in blue) and D_α (in red) overplotted; b) Te_{38} and n_e(edge); c) spectrogram of reflectometry; frequency and intensity (in magenta) of the modes identified in different frequency ranges: d) 50-100 kHz; e) 5-50 kHz. The dashed vertical red lines signal the change in the PF of the reflectometer, the 8 PFs are exposed in increasing order.

4.3. Determination of the radial profile of the mode between ELMs

The reflectometry configuration of the master channel in the discharges 86469 and 86470 permitted to follow different density layers (near the pedestal) in time intervals of 0.2 s. The spectrogram of these reflectometry's signals indicate that the mode at 70-100 kHz, mentioned in the previous chapter, is more defined in some PFs than others. This indicates that the mode is not homogeneous and varies along the radius of the tokamak. Which makes it of interest to obtain a profile of its location with an associated intensity and frequency. The profile of the mode parameters was estimated using selected intervals covering the different periods along the ELM cycle. The intervals chosen considered that the n_e profile didn't vary much, so the probed regions are assumed to stay constant. From these intervals an algorithm was implemented that took into consideration a recovery of the plasma quantities after each ELM and ignored that period.

Following these conditions allowed to choose intervals for the construction of the mode localisation. Our objective is to know for each PF used, what is the average intensity and average frequency of the mode using the selected points. To do so we want to gather these mode characteristics based on the corresponding PF of each point from the full sweeps of the selected data. Building 8 groups that have the mode intensities and frequencies of a specific PF. With all the available points for each PF, we calculate an average of the mode intensity and frequency as well as a standard deviation. By associating a corresponding radius with each PF, using the closest n_e profile, it is possible to build a profile of the mode intensity and frequency along the radius like the ones shown in figures 13 and 14.

Discharge 86469

With the chosen intervals, the mode localisation was done and presented in figure 13. In plot a), mode intensity is presented along the radius with the number of the associated PF; in plot b), the mode frequency is shown as well as the corresponding number of used points by each PF; in plot c), a density profile is presented and in plot d) are the corresponding PFs (used by the fast sweep reflectometer to determine each density). Like mentioned before, this profile was needed to locate the PFs used by the CR along a full sweep, which are annotated from 1-8 in both profiles.

The intensities of the modes clearly indicate that it is localised between the PFs 3-6, around the pedestal top and extending up to the middle of the steep density gradient region. It is located between R=3.78-3.798 m being strongest for the PF 4 at R=3.79 m. Even though the probing frequencies 1 and 2 have intensities above the considered threshold value, the mode detected has high variance in both intensity and frequency. The PSDs along these two PFs show that the identified modes are in fact broadband fluctuations of high amplitude.

In the PFs 3-6, where the mode existed, the mean frequency shows a slight decrease as the radius increases. The mode is identified with 77.6 kHz at the top of the pedestal (PF 6) and continuously goes down to 72.2 kHz at the middle of the steep gradient region (PF 3). The frequency difference between these two PFs is 5.4 kHz. An indicative mode frequency was calculated based on a weighted average frequency over the 3 most intense PFs of the mode, the weights being the corresponding mode intensities. The result is $\overline{f} = 76$ kHz.

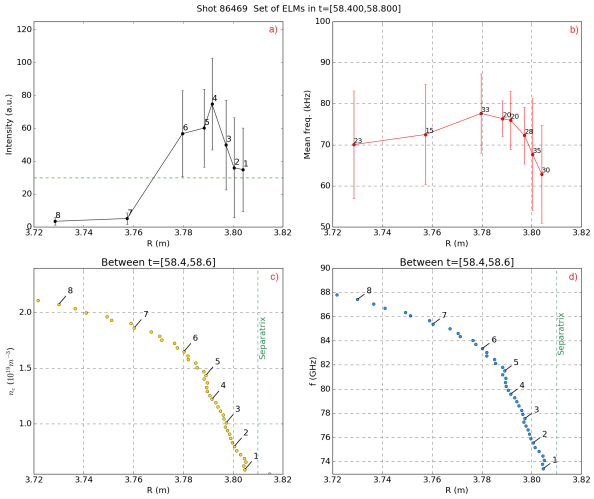

Figure 13: Profile of the mode obtained from the range 50-100 kHz. a) Intensity of the mode along the radius and PFs annotated (the green dashed line is the intensity threshold of a mode), b) mean frequency along the radius and # points used annotated, c) average electron density profile of LFS and d) Radial profile of the PF.

Discharge 86470

The resulting mode localisation for this discharge is presented in figure 14. The mode location is not as obvious for this discharge. We have two peaks along the radius, the main peak at the PFs 6 and 5 and a second peak in the PFs 2 and 3 with the 4^{th} having a lower intensity. The second peak at the PF 2 can be considered artificial since this PF has high variance in both intensity and frequency, by looking at the PSDs a set of intense broadband fluctuations are detected by the mode detection algorithm, like in the previous discharge. The intensity at the PF 4 should be at least bigger than the PF 3, assuming that there is only one mode localised around the PF 5. However, the intensity in PF 4 is lower than expected, which can be justified by the evolution along the ELM cycle. In this case the ignored time after the ELMs may not be sufficient, leading to some points where the plasma quantities are still recovering to be used. This results in an underestimation of intensity for this PF. Taking all the above into consideration, we can locate the mode around the PFs 3-7, with the PF 7 showing the mode very faintly. We can locate the mode strongly at the PF 5 at R=3.788 m, near the top of the pedestal, and is distributed across R=3.762-3.8 m, that covers the pedestal top and reaches up to the middle of the steep density gradient region.

The mean frequency profile of this discharge also shows a decreasing tendency from the top of the pedestal (PF 6) to the middle of the steep gradient region (PF 3). Although the PF 5 seems to be an outlier, its variance covers a frequency in which the trend would uphold. The mode is identified with 85.3 kHz for PF 6 and down to 80 kHz at the PF 3. Similar to the previous discharge, the difference of the mode frequency between the most distant layers where it was identified more strongly is 5.3 kHz.

The same indicative calculation of a weighted average frequency was done for this mode with the 3 most intense PFs, ignoring the PF 2 due to the reasons mentioned before. From this calculation we have that the mode has $\overline{f} = 81$ kHz.

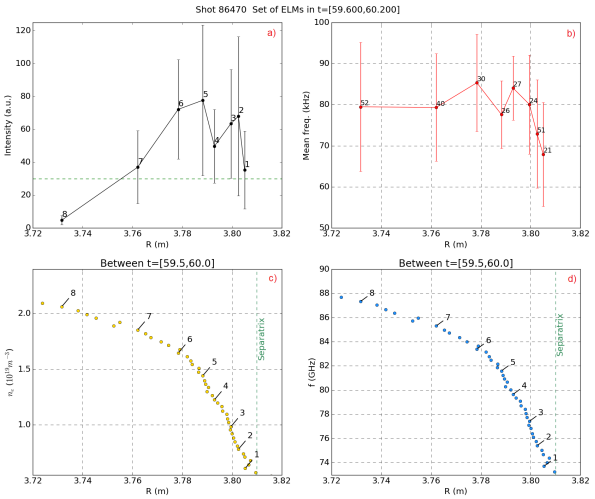

Figure 14: Profile of the mode obtained from the range 50-100 kHz

The frequency difference between the most distant mode layers being about 5 kHz for both discharges corroborates the explanation given for the observed frequency shift between the CR and the magnetic coils of the discharge 84733. The CR was probing a density layer at the pedestal top, identifying a mode with increased frequency. While the measured fluctuations in the magnetic coils, which should be caused mainly by the outer layers, have the same mode at a smaller frequency with a 5 kHz shift.

By comparing the resulting mode frequencies from these two discharges, the #86469 at $\overline{f} = 76$ kHz and the the #86470 at $\overline{f} = 81$ kHz. These are very similar frequencies which indicate that it is the same mode. The frequency discrepancy between them can be justified by the difference in the P_{NBI} being used in the selected points that caused the plasma to rotate faster. In terms of mode location they are consistent between discharges with the mode being at R=3.78-3.798 m for #86469 and at R=3.762-3.8 m for the #86470, with the maximum of the mode intensity being concordant at R=3.788 m and R=3.79 m, respectively.

5. Conclusions

The objective for this thesis was to make an analysis of an instability at the edge of the plasma that seemed to be correlated with ELM events. The mode had a frequency range of [60-90] kHz and was detected and monitored in three discharges using correlation reflectometry. We were able to relate its intensity with the recovery of edge density after the ELM. We also determined the mode position between ELMs by varying the probing frequency of the reflectometer in a pre-determined pattern, which allowed to scan multiple density layers of the plasma.

Many tools were developed to facilitate the analysis of

the different discharges that allowed for a better understanding of the mode behaviour, leading to many observations and results that are worth remarking. An intermittent behaviour of the mode was observed in the correlation reflectometry signal for the different discharges and was attributed to low frequency oscillations in the D_α that would reduce the overall activity in the power spectrum. We noted that the mode of interest had a magnetic nature, appearing whenever these ocillations would vanish. In these intervals of low D_α activity, we compared the modes observed in the magnetic and reflectometry signals and a frequency shift of the mode by about 5 kHz to smaller values was detected in the magnetic mode, attributed to different rotation velocities in the plasma. The mode was only visible in the magnetic signals of the low field side, indicating a ballooning structure.

The mode intensity variation, in the discharge measuring a fixed layer, for periods with low density was discovered to be caused by the position of the correlation reflectometer. By probing at the top of the steep gradient region when the densities were higher, whenever these densities would drop, the region being probed changed to more inside the plasma, a region where the mode did not exist. After each ELM we suspect this change in scanning region also happened justifying the correlation found between the mode intensity and edge density. However, this correlation after the ELM is also present in the discharges measuring in multiple layers. Indicating the mode intensity is in fact correlated with the density gradient. The temperature at the top of the pedestal usually recovered much faster that the n_e and mode intensity, although there were some cases where the temperature was more correlated to the mode intensity than the n_e.

A particular behaviour that is worth noticing is that mode frequency seems to vary with the heating power of neutral beam injection, P_{NBI}, along the discharges. An increase or decrease in heating power results in the modes of both reflectometry and magnetic coils to respectively increase or decrease in frequency. This dependence of the mode frequency on the heating power is justified by the change in the rotation of the plasma. This translates to the layer where the mode exists to rotate faster, increasing the mode frequency.

In all discharges, another mode was identified around 10-20 kHz both in the reflectometry and magnetic signals associated with sawtooth events. This mode, when strongest in the reflectometry signal, affected the intensity of the mode of interest by reducing its intensity. This phenomenon could be justified by a magnetic instability associated with sawteeth that interferes with the main mode but further studies are needed.

Along the discharges with measurements in multiple layers, the main mode was observed in the steep gradient region around R=3.78-3.80 m. We were able to successfully localise the mode using the developed algorithm that determined its intensity and frequency along the radius. The mode was identified to have a frequency of $\overline{f} = 76$ kHz, and located at R=3.78-3.798 m for one of the discharges and with $\overline{f} = 81$ kHz and located at R=3.762-3.8 m for the other. The frequency profile obtained from these radial discharges helped understand the frequency shift of the main mode observed between the CR and the magnetic coils for the discharge probing a single layer.

In summary, with this work we were able to describe the mode evolution probing a single layer of the plasma as well as show how hopping reflectometry can help determine the localisation of a mode along the radius. In future work, radial location of the mode in periods without ELMs could be explored complemented with more density profiles. This way we could correlate the mode intensity with the steepness of the density gradient at different points of the discharge. The density profiles could also be explored with more detail using a mtanh fit that would help identify with more precision the pedestal width and height, and use these to compare to the EPED model. Also, a further analysis using the phase and the amplitude separated could be done to check if the observations done with the complex signal I+jQ translate to each of these quantities.

Acknowledgements

Many thanks to my supervisor Carlos Silva, for helping me throughout my work, to my friends for keeping me company online and helping me clear my mind and to my parents for providing a welcoming home and being supportive throughout this long project.

References

[1] G. Birkenmeier et al. Magnetic structure and frequency scaling of limit-cycle oscillations close to l- to h-mode transitions. *Nuclear Fusion*, 56(8):086009, jul 2016.

[2] J. C. Hillesheim et al. Stationary zonal flows during the formation of the edge transport barrier in the jet tokamak. *Physical Review Letters*, 116(6), 2 2016.

[3] F. M. Laggner. *Inter-ELM pedestal structure development in ASDEX Upgrade*. PhD thesis, Technischen Universität Wien, 2017.

[4] C. Maggi et al. L-h power threshold studies in jet with be/w and c wall. *Nuclear Fusion*, 54, 01 2014.

[5] M. Nave, B. Alper, D. Borba, C. Boswell, C. Challis, M. Brix, S. Gerasimov, S. Hacquin, N. Hawkes, E. Joffrin, J. Mailloux, E. de la Luna, and P. Smeulders. On the use of mhd mode analysis as a technique for determination of q-profiles in jet plasmas. *Review of Scientific Instruments*, 75, 10 2004.

[6] C. Silva, J. Hillesheim, C. Hidalgo, E. Belonohy, E. Delabie, L. Gil, C. Maggi, L. Meneses, E. Solano, M. Tsalas, and et al. Experimental investigation of geodesic acoustic modes on jet using doppler backscattering. *Nuclear Fusion*, 56(10):106026, 2016.

[7] H. Zohm. Edge localized modes (ELMs). *Plasma Physics and Controlled Fusion*, 38(2):105–128, 02 1996.